A HIGH RESOLUTION GLOBAL OCEAN MODEL with VARIABLE FORCING of WIND, HEAT, and FRESHWATER: II) TRANSPORT VARIABILITY

Robin Tokmakian, Naval Postgraduate School, Monterey, CA 93943 USA robint@ucar.edu

Goal: Understand ocean's low freq. variability

Conclusions in Red

Model Simulation Details:

(Semtner & Chervin '92, Stammer, et al. '96, Tokmakian, '96)

- 1/4°avg. Semtner/Chervin Primitive Eq. OGCM
- Parallel Ocean Climate Model POCM-vers 4C
- Forced with ECMWF reanalysis + oper. 1979-1996
  --> heat, freshwater, wind stress - varying daily (including rivers)

Meridional Heat Flux

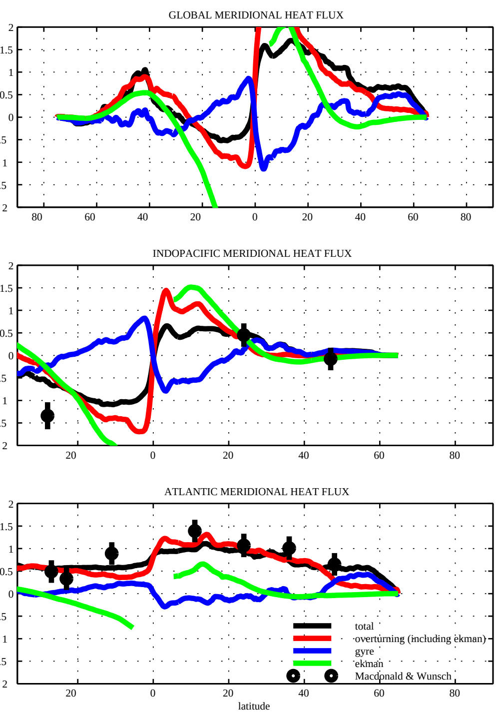

Calculated from monthly means

Overturning, where <> is mean

$\rho * C_p \int_H \left[L \langle V_{zonal} \rangle \langle T_{zonal} \rangle \right] dz$,

Gyre

$\rho * C_p \int_H \int_L (V - \langle V \rangle)(T - \langle T \rangle) d\lambda dz$

Ekman

$C_p \int_L -\tau^x / f (T_{surface} - \langle T_{zonal} \rangle) d\lambda$

Long Term Mean

POCM 4C simulates the mean heat flux well as compared to Macdonald & Wunsch ('96).

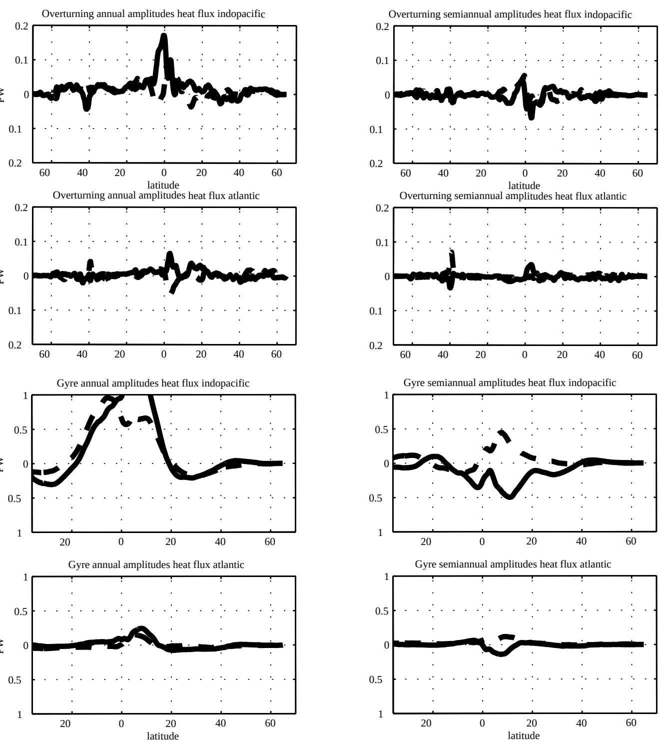

The plots to the left show the amplitudes of the annual and semi-annual signals for the components of the heat flux in the Indo-Pacific and the Atlantic regions.

The annual cycle is 8% of the total HF at 24°N in the overturning component; 30% of total for the gyre component at 24°N; semi-annual contributes less than 1%.

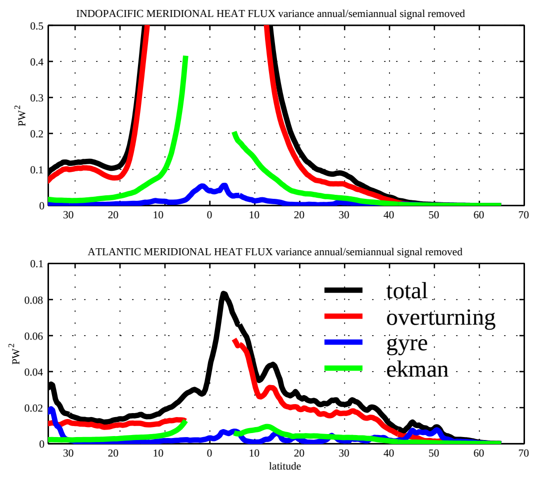

The diagram to the left shows the variance in the heat flux with the annual and semi-annual signal removed, for each component.

Indo-Pacific Meridional Heat Flux

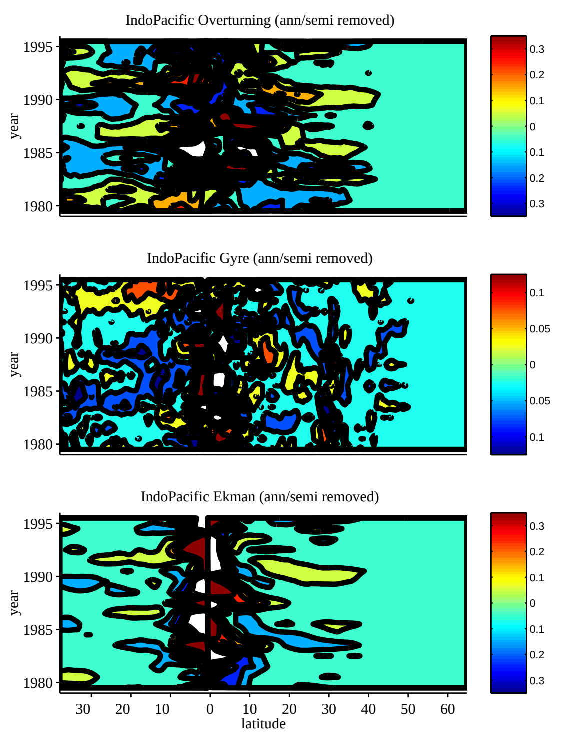

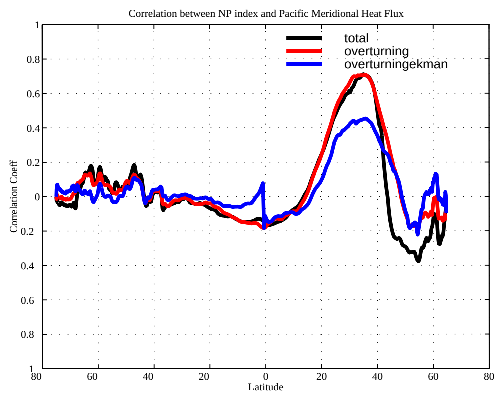

Above the correlation of the North Pacific Index (Trenberth & Hurrell, '94, mean SLP 30°->65°N & 160°E ->140°W). The high corr. region corresponds to where ekman flux contributes 30% or more to the variability.

Time-latitude plots are shown for the components of heat flux. Note, the annual and semi-annual signal has been removed and the ekman component is included in the overturning component. Low frequency variability > annual is clearly simulated by the model visible in these integrated quantities. (Contours: gyre 0.05 PW, other 0.1PW).

At 24°N, the top 400 m contribute most to the variability of the overturning.

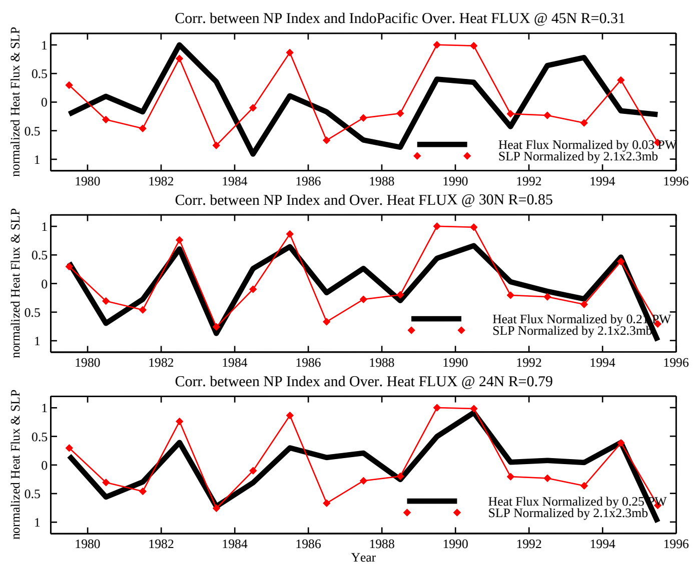

Shown at left are normalized time-series of the NP index (with annual/semi-annual signal removed) and the meridional heat flux at three latitudes, 45°, 30°, & 24°N.

Maximum variability is on theorder of 0.4 PW at 24°N, & the monthly minimum is found in the during spring/ summer.

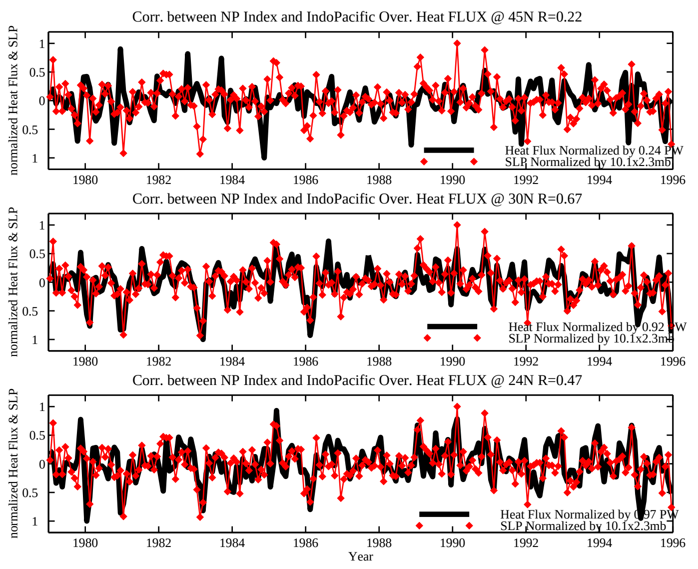

@24°N; total HF in Pacific can be separated as:

Ekman =	*0.38 PW*
Kuroshio (gyre) =	*-0.026PW*
Kuroshio (over.) =	*2.4PW*
Mid-ocean (gyre)=	*-0.03PW*
Mid-ocean (over)=	*-2.24PW*
	0.48 PW

Atlantic Meridional Heat Flux

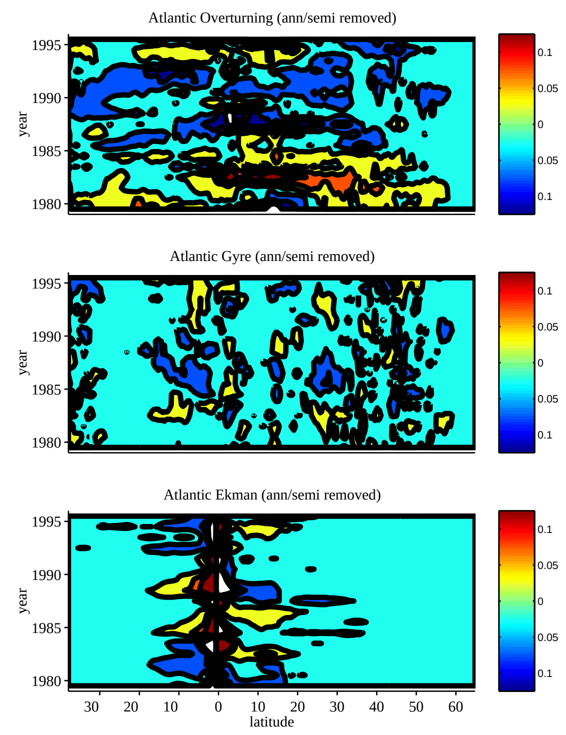

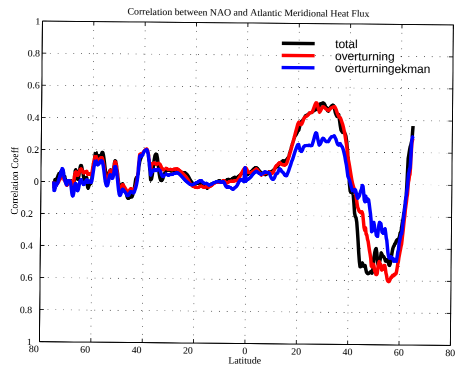

Above is the correlation of the North Atlantic Oscil. Index - NAO (Hurrell, '95, SLP diff Azores & Iceland).

<---(Contours are 0.05PW.)

Time-latitude plots are shown for the components of heat flux. Note, the annual and semi-annual signal has been removed and the ekman component is included in the overturning component.

The ekman flux contributes little to the overturning heat flux north of 40°N.

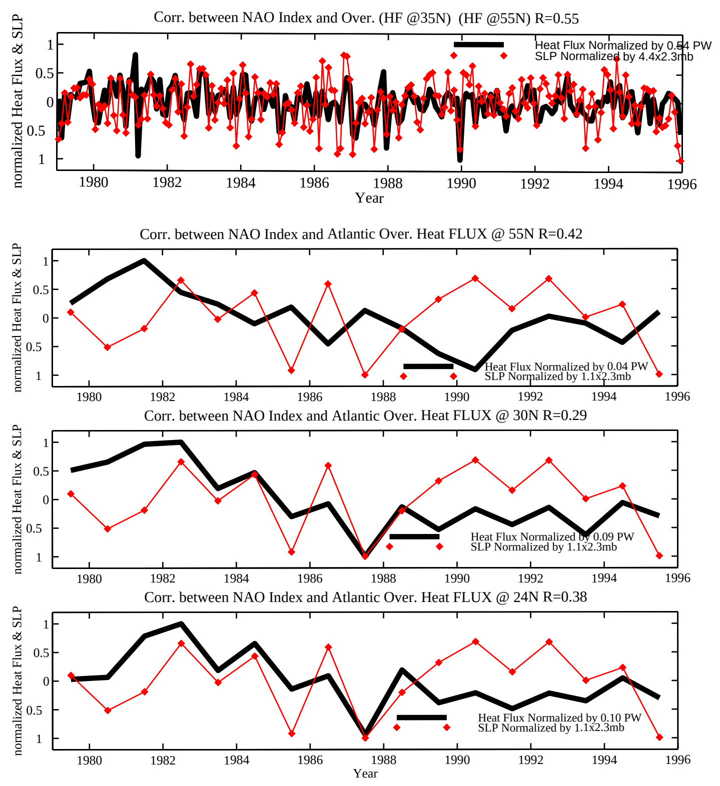

A time-series of the NAO index (with annual/ semi-annual signal removed) and the difference in the meridional heat flux at 35°N and 55°N (because NAO is a difference in SLP). This shows the relative influence of atmospheric conditions on the overturning heat flux of the model.

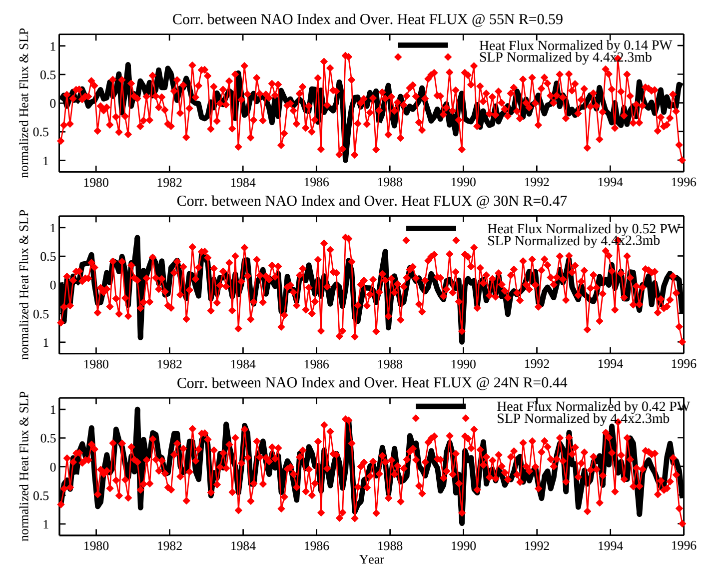

To the left are normalized time-series of the NAO index (with annual/ semi-annual signal removed) and the meridional heat flux at three latitudes, 55°, 30°, & 24°N.

Maximum annual variability is on the order of 0.2 PW at 24°N, & the monthly variability also 0.2 PW.

Meridional Salt & Freshwater Fluxes

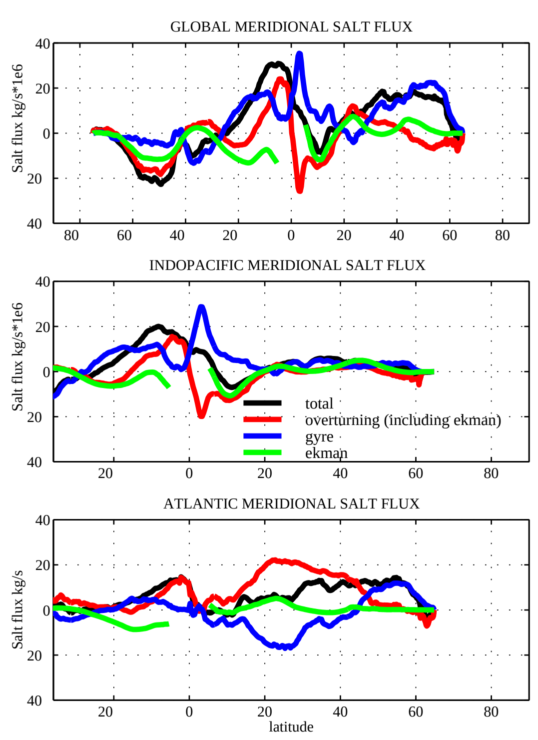

The salt flux calc. follow the heat flux calc. above, replacing T with S, & changing the constant to ρ only.

Freshwater Calc. (mass flux minus %which is salty)

$\rho(\langle v \rangle - \langle v \rangle \langle S \rangle - \langle v'S' \rangle)$

(Arctic inflow/outflow included at 60°N.)

Plot to right shows the freshwater trans. in the model as compared to Wijffels '92. The model does not simulate the northward flux of Antarctic water correctly

N. Atlantic & Indo-Pacific fluxes are similar to observations

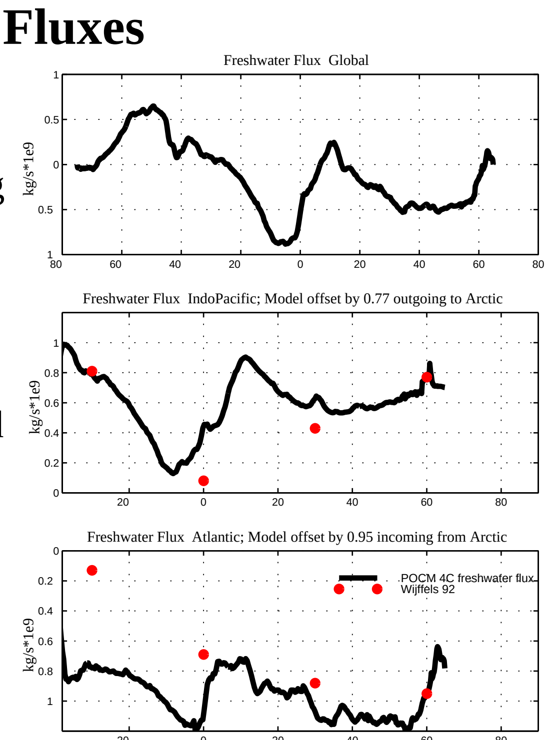

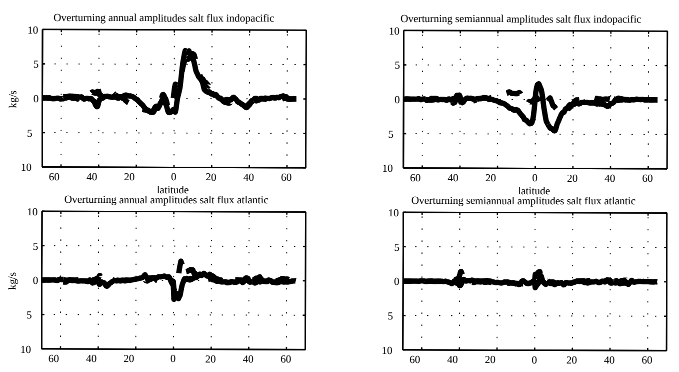

The plots to the right & left show the amplitudes of the annual and semi-annual signals for the components of the salt flux in the Indo-Pacific and the Atlantic regions.

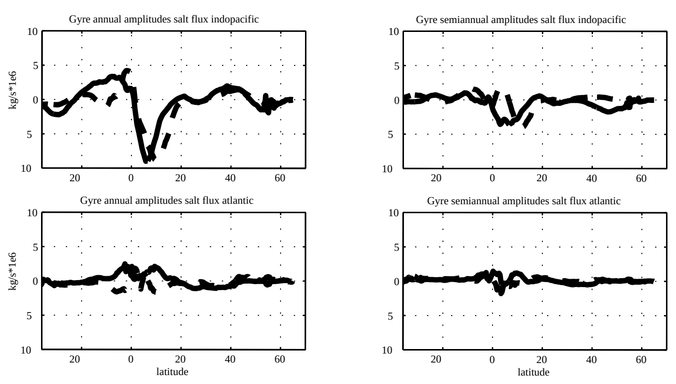

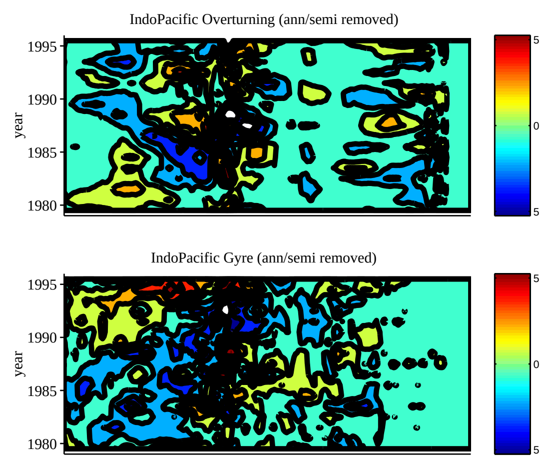

The variablility with time of the salt flux for the Indo-Pacific and the Atlantic with the annual/semi-annual signal removed shows that the *overturning and gyre components contribute equally to the total* salt flux, especially in the S. Pacific and the Atlantic. Contours are 1.5 kg/s*1e6: Indo-Pac; kg/s*1.e6 for Atl.

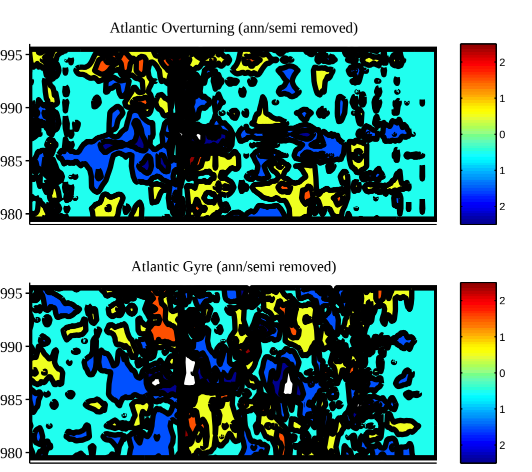

Acknowledgements: Funding provided by NSF-WOCE, DOE, under CHAMMP; Computer resources provided by NCAR. Thanks to H. Bryden, B. Semtner for suggestions for this research.